Research Square

Preprints are preliminary reports that have not undergone peer review.
They should not be considered conclusive, used to inform clinical practice,
or referenced by the media as validated information.

Uncoupling HIF-1α/ABCB1 signaling from chemoresistance: Intermittent hypoxia sensitizes breast cancer to 5-Fluorouracil and Doxorubicin combination therapy in vitro and in vivo

Hayarpi Javrushyan

hg.javrushyan@ysu.am

Yerevan state university

Nikolay Avtandilyan

Yerevan state university

Edita Nadiryan

Yerevan State University

Alina Maloyan

OHSU, Portland, USA

Article

Keywords: Breast cancer, Intermittent hypoxia, Tumor microenvironment, Chemoresistance, HIF-1α, Apoptosis, Doxorubicin, 5-Fluorouracil, DMBA-induced mammary carcinoma, Hypoxic conditioning

Posted Date: July 30th, 2026

DOI: https://doi.org/10.21203/rs.3.rs-10282354/v1

License: This work is licensed under a Creative Commons Attribution 4.0 International License.
Read Full License

Additional Declarations: There is no conflict of interest

Uncoupling HIF-1α/ABCB1 signaling from chemoresistance: Intermittent hypoxia sensitizes breast cancer to 5-Fluorouracil and Doxorubicin combination therapy *in vitro* and *in vivo*

Nikolay Avtandilyan[1], Edita Nadiryan[1], Alina Maloyan[2], Hayarpi Javrushyan[1*]

[1] Research Institute of Biology, Yerevan State University, Alex Manoogian, Yerevan, Armenia.

[2] Center for Developmental Health, Knight Cardiovascular Institute, Oregon Health & Science University, Portland, USA.

Nikolay Avtandilyan: nv.avtandilyan@ysu.am

Edita Nadiryan: edita.nadiryan@ysu.am

Alina Maloyan: alina.maloyan@gmail.com

Hayarpi Javrushyan: hg.javrushyan@ysu.am*

***Corresponding author: Dr. Hayarpi Javrushyan, PhD**

Yerevan State University, 1 Alex Manoogian, Yerevan, RA, 0025; Phone: (+37460) 710520

E-mail: *Hayarpi Javrushyan: hg.javrushyan@ysu.am

ORCID number: **https://orcid.org/0000-0002-6941-8283**

Abstract

Hypoxia is a defining feature of the tumor microenvironment and is classically associated with chemoresistance through HIF-1α-driven adaptive signaling. However, whether mild intermittent oxygen fluctuation, rather than chronic severe hypoxia, can sensitize breast cancer cells to chemotherapy remains unclear. Here, we investigated the effects of mild intermittent hypoxia on tumor progression and chemosensitivity using complementary in vitro and in vivo models.

In SKBR3 and MDA-MB-231 breast cancer cells, hypoxia was chemically induced with $CoCl_2$ (100–300 μM), while TNF-α was added to mimic the inflammatory component of the tumor microenvironment, thereby recreating hypoxic and inflammatory conditions associated with the development of chemotherapy resistance. Under these conditions, HIF-1α and ABCB1 (P-glycoprotein), a major ATP-dependent drug efflux transporter implicated in multidrug resistance, were upregulated in a concentration-dependent manner, and this hypoxia-associated response persisted following co-treatment with the chemotherapeutic agents doxorubicin (DOX) and 5-fluorouracil (5-FU). Notably, cells exposed to moderate hypoxia (200 μM $CoCl_2$) together with DOX/5-FU exhibited the greatest activation of apoptosis, as demonstrated by increased caspase-3 expression accompanied by reduced GLUT-1 expression, indicating enhanced chemotherapy-induced cytotoxicity under controlled hypoxic conditions.

To evaluate these findings in vivo, mammary tumors were induced in rats using 7,12-dimethylbenz[a]anthracene (DMBA), a well-established model that recapitulates key pathological and molecular features of human breast cancer. Intermittent mild hypoxia (13% O_2, cyclic exposure) alone increased tumor size approximately twofold and upregulated HIF-1α, ABCB1 (P-glycoprotein), and BCL-2 compared with rats bearing DMBA-induced tumors maintained under normoxic conditions, consistent with activation of hypoxia-associated pro-survival pathways. In contrast, combining intermittent hypoxia with DOX/5-FU chemotherapy significantly reduced tumor growth compared with both the hypoxia-only and chemotherapy-only groups and produced the strongest caspase-3-associated apoptotic response.

Kaplan–Meier survival analysis demonstrated a significant survival benefit of chemotherapy irrespective of oxygenation status (log-rank $p = 0.0387$), while body weight measurements indicated no evidence of treatment-related systemic toxicity.

Collectively, these findings demonstrate that although mild intermittent hypoxia alone promotes pro-survival signaling characteristic of the hypoxic tumor microenvironment, its combination with chemotherapy enhances apoptotic cell death and suppresses tumor growth. These results support the concept that controlled hypoxic conditioning can remodel the tumor microenvironment in a manner that improves responsiveness to cytotoxic therapy, providing a potential strategy for overcoming hypoxia-associated chemoresistance in breast cancer.

Keywords

Breast cancer; Intermittent hypoxia; Tumor microenvironment; Chemoresistance; HIF-1α; Apoptosis; Doxorubicin; 5-Fluorouracil; DMBA-induced mammary carcinoma; Hypoxic conditioning

Highlights

- Mild intermittent hypoxia induces a HIF-1α–driven pro-survival program in breast cancer cells, including upregulation of ABCB1 and BCL-2.
- Hypoxic preconditioning alone enhances tumor growth and inflammatory signaling, but does not confer resistance to 5-fluorouracil/doxorubicin (FUDOX) chemotherapy.
- Moderate hypoxic exposure ($CoCl_2$ 200 μM) maximizes chemotherapy-induced caspase-3 activation, indicating a biphasic, hormetic response.
- In vivo, intermittent hypoxia combined with FUDOX significantly reduces tumor burden and improves survival in DMBA-induced mammary carcinoma without systemic toxicity.
- Hypoxia-driven tumor adaptation is partially reversed by chemotherapy, leading to suppression of HIF-1α/ABCB1 signaling and activation of apoptotic pathways.

Abbreviations: ABC, ATP-binding cassette; ABCB1 (P-gp/MDR1), ATP-binding cassette subfamily B member 1 (P-glycoprotein); ABCG2, ATP-binding cassette subfamily G member 2; AKT, protein kinase B; ANOVA, analysis of variance; ATCC, American Type Culture Collection; ATP, adenosine triphosphate; AUC, area under the curve; BCA, bicinchoninic acid; BCL-2, B-cell lymphoma 2; BSA, bovine serum albumin; $CoCl_2$, cobalt chloride; DAPI, 4′,6-diamidino-2-phenylindole; DMBA, 7,12-dimethylbenz[a]anthracene; DMEM, Dulbecco's Modified Eagle Medium; DMSO, dimethyl sulfoxide; DOX, doxorubicin; ECL, enhanced chemiluminescence; ELISA, enzyme-linked immunosorbent assay; ERK1/2, extracellular signal-regulated kinase 1/2; 5-FU, 5-fluorouracil; FUDOX, combined 5-fluorouracil and doxorubicin treatment; GLUT-1, glucose transporter 1; HER2, human epidermal growth factor receptor 2; HIF-1α, hypoxia-inducible factor 1-alpha; HRP, horseradish peroxidase; ICC, immunocytochemistry; IF, immunofluorescence; IHC, immunohistochemistry; KEGG, Kyoto Encyclopedia of Genes and Genomes; MAPK, mitogen-activated protein kinase; mTOR, mechanistic target of rapamycin; NF-κB, nuclear factor kappa-light-chain-enhancer of activated B cells; PBS, phosphate-buffered saline; PFA, paraformaldehyde; PI3K, phosphoinositide 3-kinase; RIPA, radioimmunoprecipitation assay buffer; RTCA, real-time cell analysis; SD, standard deviation; TBST, Tris-buffered saline with Tween 20; TME, tumor microenvironment; TNF-α, tumor necrosis factor-alpha; VEGF, vascular endothelial growth factor; WB, Western blot.

1. INTRODUCTION

Breast cancer remains a major cause of cancer-related morbidity and mortality worldwide, and resistance to chemotherapy continues to limit long-term therapeutic success [1,2]. Increasing evidence indicates that the tumor microenvironment plays a pivotal role in shaping treatment response, with oxygen availability emerging as one of its most influential components [3,4]. Hypoxia is a hallmark of solid tumors and contributes to malignant progression through activation of hypoxia-inducible factor-1α (HIF-1α), a transcription factor that orchestrates cellular adaptation to low oxygen tension [5–8]. Through HIF-1α-dependent signaling, hypoxic tumors upregulate genes involved in glycolytic metabolism, stress adaptation, angiogenesis, cell survival, and drug resistance, including glucose transporter 1 (GLUT1) and ATP-binding cassette subfamily B member 1 (ABCB1/P-glycoprotein) [9], while simultaneously modulating apoptotic pathways through regulators such as BCL-2 and caspase-3 [10–12].

Although chronic hypoxia has been extensively investigated in cancer biology, intermittent hypoxia may exert distinct biological effects because it exposes cells to repeated cycles of oxygen deprivation and reoxygenation rather than sustained oxygen shortage [13–15]. Such fluctuations can generate reactive oxygen species, induce oxidative stress, and trigger unique transcriptional programs that differ from those elicited by chronic hypoxia [16]. In breast cancer, intermittent hypoxia has been associated with enhanced invasiveness, glycolytic reprogramming, metastatic gene expression, acquisition of stem-like

characteristics, and activation of signaling pathways linked to therapeutic resistance [7,11,17,18]. However, these observations have predominantly been derived from experimental models that employ severe hypoxia-reoxygenation cycles to mimic unstable tumor perfusion. Importantly, the biological consequences of intermittent hypoxia appear to depend critically on the severity, duration, frequency, and pattern of oxygen fluctuation [13,14,17]. While severe cyclic hypoxia is generally regarded as tumor-promoting, controlled mild intermittent hypoxia has emerged in other pathological contexts as a form of hypoxic conditioning capable of inducing adaptive and potentially protective responses. This phenomenon, often referred to as hypoxic hormesis, has been associated with improved cardiovascular, metabolic, and neurological outcomes through activation of endogenous defense mechanisms and enhancement of stress resistance [7,13–15]. Therefore, the harmful effects of severe cyclic hypoxia are well documented, whereas the consequences of controlled mild intermittent hypoxia during cancer treatment remain poorly understood [5,10,19]. These observations raise an important question: can mild intermittent hypoxia reshape the tumor microenvironment in a manner that enhances responsiveness to chemotherapy rather than promoting resistance? Controlled oxygen fluctuation may not simply recapitulate the effects of chronic tumor hypoxia [5,11,20]. Instead, low-dose intermittent hypoxia could potentially influence the balance between survival and apoptotic pathways, modify inflammatory and metabolic responses, alter drug-efflux mechanisms, and increase the susceptibility of tumor cells to chemotherapy-induced cell death [5,13]. To address this question, the present study investigated the effects of intermittent mild short-term hypoxia in a DMBA-induced rat model of breast cancer. We evaluated whether the combination of mild intermittent hypoxia with conventional chemotherapy modulates tumor burden and key biomarkers associated with hypoxic signaling, metabolic adaptation, apoptosis, inflammation, and chemoresistance, including HIF-1α, GLUT1, ABCB1, BCL-2, caspase-3, and TNF-α [4,9,21–23]. By examining the interaction between controlled oxygen fluctuation and chemotherapy, this study aims to determine whether mild intermittent hypoxia can shift the tumor microenvironment toward a more treatment-responsive phenotype.

2. MATERIALS AND METHODS

2.1. Materials

Chemicals for cell culturing and breast cancer induction were purchased from Sigma-Aldrich (USA) and Abcam. TNF-α (ab100785), rat ELISA kits, and antibodies HIF1a (ab179483), BCL-2 (ab194583), Caspase-3 (ab184787), GLUT-1 (ab115730), and ABCB-1 (ab170904 for WB, IHC, and ab235954 for ICC/IF), Goat anti-rabbit IgG HandL (Alexa Fluor488, ab150077; Alexa Fluor647, ab150115), anti-beta actin (ab8227), and anti-rabbit IgG HandL (HRP, ab6721) for WB and ICC/IF, IHC/IF were purchased from Abcam. Cell culture reagents, including culture media, antibiotics/antimycotics, amino acids, glutamine, and related supplements, were obtained from Thermo Fisher Scientific and Gibco.

2.2. Cell culture

Human breast cancer cell lines MDA-MB-231 (ATCC® HTB-26™) and SK-BR-3 (ATCC® HTB-30™) were kindly provided by the L.A.Orbeli Institute of Physiology, NAS RA (Yerevan, Armenia). The cell lines were originally obtained from the American Type Culture Collection (ATCC, Manassas, VA, USA). Cells were maintained in DMEM supplemented with L-glutamine (2 mmol/L), sodium pyruvate (200 mg/L), fetal bovine serum (10%, v/v), and antibiotics (100 U/mL penicillin and 100 µg/mL streptomycin). Cultures were grown at 37°C in a humidified atmosphere containing 5% CO_2 in a PHCbi incubator (Japan), as previously described [24,25].

2.3.Experimental groups

The experimental design was intended to evaluate the effects of chemotherapy under conditions simulating hypoxia-associated and inflammatory tumor microenvironments. To mimic hypoxic and inflammatory conditions characteristic of the tumor microenvironment (TME), MDA-MB-231 and SK-BR-3 cells were seeded and allowed to attach overnight under standard culture conditions. The following experimental groups were generated for this study: MDA-MB-231 and SK-BR-3 cells were plated in a 96-well black cell culture microplate and incubated for 24 h. For ICC analysis, the groups were: (1) Control cells (DMSO), (2) Cells + 10 ng/ mL TNFα + 100 µM CoCl2, (3) Cells + 10 ng/ mL TNFα + 200 µM CoCl2, (4) Cells + 10 ng/ mL TNFα + 300 µM CoCl2, (5) Cells + 10 ng/ mL TNFα + 100 µM CoCl2+10 µM 5FU+0.1 µM DOX, (6) Cells + 10 ng/ mL TNFα + 200 µM CoCl2+10 µM 5FU+0.1 µM DOX (7) Cells + 10 ng/ mL TNFα + 300 µM CoCl2+10 µM 5FU+0.1 µM DOX. TNF-α and CoCl2 were applied with the treatment (10 µM 5FU+0.1 µM DOX). The cells were then incubated for 24 h, followed by fixation.

2.4.In Vitro Chemical Hypoxia and Inflammatory Tumor Microenvironment Model

Twenty-four hours after plating, cells were exposed to cobalt chloride ($CoCl_2$) at concentrations of 100, 200, or 300 µM to induce chemical hypoxia. In parallel, recombinant TNF-α (10 ng/mL) was used to simulate the inflammatory component of the tumor microenvironment. To account for the potential intrinsic biological effects of each stimulus, appropriate control groups were included, consisting of untreated cells, $CoCl_2$-only treated cells, and TNF-α-only treated cells. For combination treatment, cells were simultaneously exposed to $CoCl_2$ and TNF-α, followed by treatment with chemotherapeutic agents 5-fluorouracil (5-FU, 10 µM) and doxorubicin (DOX, 0.1 µM) to assess chemosensitivity under conditions mimicking a hypoxic and inflammatory tumor microenvironment. After an additional 24 h incubation period, cells were processed for immunocytochemical analysis of HIF-1α, GLUT-1, ABCB1, and Caspase-3 expression. To distinguish treatment-specific effects, $CoCl_2$-only and TNF-α-only groups were analyzed in parallel, while the primary focus of the study was the combined hypoxia–inflammation

condition, which more closely reflects the in vivo tumor microenvironment and was therefore carried forward for direct comparison with the in vivo intermittent hypoxia model.

2.5.Immunocytochemistry (ICC)

Cells were fixed with 4% PFA, permeabilized with 1% Triton X-100, blocked with 1% BSA, and incubated with primary antibody (Caspase-3 1:250, ABCB-1 1:250, HIF1-a 1:250) at 4°C overnight. Then, cells were incubated with green fluorescence-labeled secondary antibody (anti-rabbit IgG HandL (Alexa Fluor488 and 647) 1:500), and nuclei were blue-stained with Hoechst (Sigma). Images were visualized on a Cytation C10 (BioTek, Agilent, USA) confocal microscope at room temperature using a 20× objective and acquired with Gen5 software (BioTek, USA), which was also used for image analysis[25].

2.6. Real-time cell analysis (RTCA)

Cell proliferation and chemosensitivity were monitored in real time using the xCELLigence RTCA eSight system (Agilent Technologies), which combines continuous impedance-based cell index measurements with automated phase-contrast imaging. SKBR-3 cells were seeded at 20,000 cells/well and MDA-MB-231 cells at 10,000 cells/well in E-Plate and allowed to attach and proliferate under standard culture conditions (37 °C, 5% CO_2) [25]. Baseline cell index was recorded for approximately 28 h before treatment. Chemical hypoxia was induced by addition of $CoCl_2$ at concentrations of 100, 200, or 300 μM in combination with TNF-α (10 ng/mL). In the combination treatment groups, cells were subsequently exposed to FUDOX (5-fluorouracil + doxorubicin) chemotherapy at the indicated time point (marked by an arrow in the cell index plots). Control wells received vehicle alone, and a separate group received FUDOX treatment without prior hypoxic conditioning. Cell index values were recorded continuously for 48 h and normalized to the pre-treatment baseline; area under the curve (AUC) was calculated for each well across the full monitoring period. Phase-contrast images were acquired automatically by the integrated eSight imaging module at the experimental endpoint using a ×10 objective; scale bars represent 100 μm. All experiments were performed with three technical replicates per condition, and each biological replicate value represents the mean of these three technical replicates; data are presented as mean ± SD of n = 4 biological replicates.

2.7.Animals and experimental groups

The experimental procedures involving animals followed Directive 2010/63/EU, and ethical approval was obtained from the Armenian National Center of Bioethics. Female albino rats (120–150 g) were randomly allocated into six experimental groups. Animals (6 animals in each group) were housed in standard cages (3500 cm^2) under controlled conditions (25°C; 12-h light/12-h dark cycle; 50–55%

humidity) and maintained on a constant diet and environment (Animal Care House, Faculty of Biology, YSU) [25,26]. Sixty-day-old rats were acclimatized for 7 days and then injected subcutaneously into the second mammary gland pair with 25 mg 7,12-dimethylbenz[a]anthracene (DMBA) dissolved in 1 mL soybean oil (Day 0). Tumor development was monitored weekly, with palpable tumors appearing approximately five weeks post-induction. Therapeutic interventions were initiated at week 6 after tumor establishment. Animals were assigned to six groups and subjected to a combined hypoxia–chemotherapy regimen. Mild normobaric hypoxia (13% O_2) was applied for 2 hours in a VelO2x hypoxic chamber (I&L Biosystems GmbH). On the following day, animals received an intraperitoneal injection of 5-fluorouracil (10mg/kg FU) and doxorubicin (0.1mg/kg DOX), followed by a rest day. This 3-day cycle was repeated six times (**Figure 1**). Animals were monitored daily for body weight, tumor progression, and general health status. At the end of the experiment, animals were humanely euthanized, and tumor and organ tissues were collected for further histological and molecular analyses.

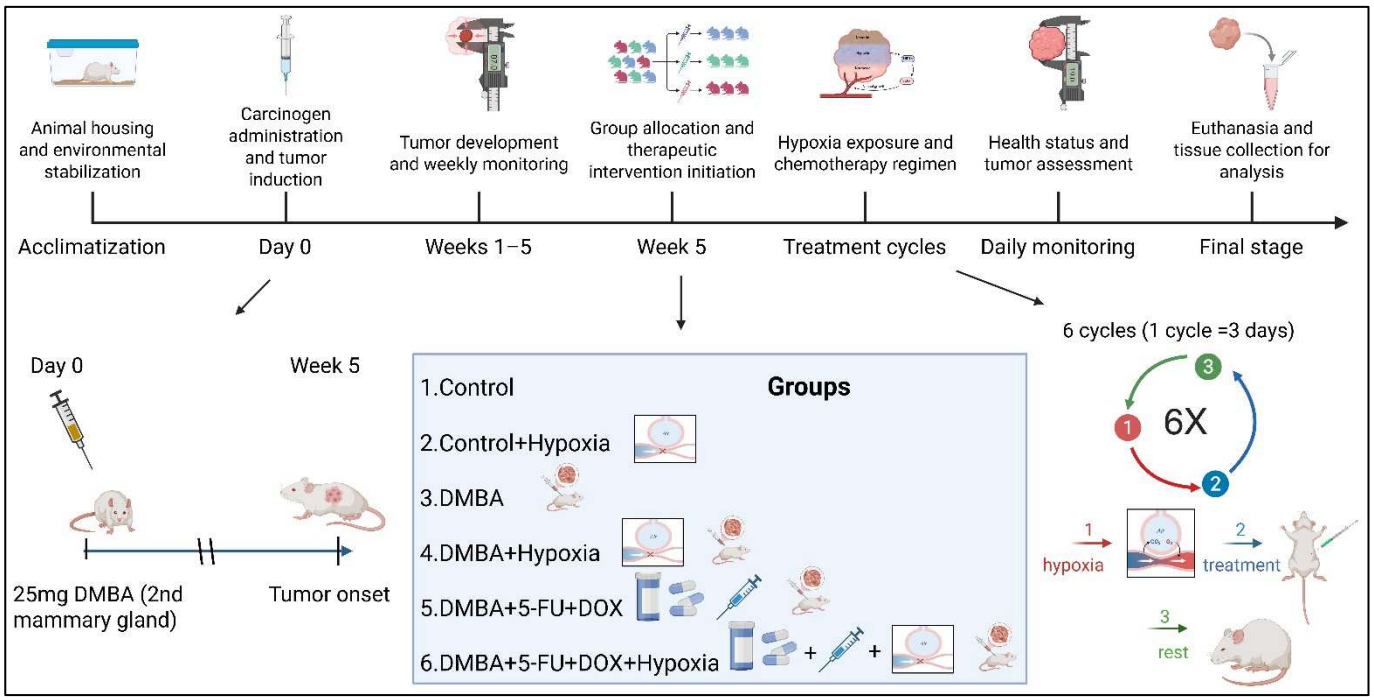


Figure 1. Animal experimental model. 7,12-dimethylbenz[a]anthracene (DMBA) was administered as a single subcutaneous injection (25 mg). Hypoxia refers to normobaric hypoxic exposure (13% O_2) for 2 hours using a VELOX hypoxic chamber (Baker Ruskinn). Each experimental group consisted of six rats.

2.8.Western Blots

About 50mg of rat tumor tissue was homogenized in RIPA buffer supplemented with a protease and phosphatase inhibitor cocktail (Abcam). Total protein concentrations were determined using bicinchoninic acid (BCA) (Bio-Rad Laboratories). Total proteins (20 µg) were separated on 4%–20% precast linear gradient gels (Bio-Rad Laboratories), transferred to nitrocellulose membranes, and

blocked with 5% (w/v) nonfat milk in TBST for 1 h. Membranes were incubated overnight at 4°C with the primary antibody (HIF1a 1:1000, BCL-2 1:2500, ABCB-1 1:1000, β-actin 1:2500) diluted in 1% nonfat milk (w/v) in TBST and detected using an appropriate peroxidase-conjugated secondary antibody (anti-rabbit IgG HandL (HRP) 1:10000). Products were visualized by ECL chemiluminescence (Millipore). Band intensities were measured using the Chemidoc (Bio-Rad Laboratories). ImageLab software was used to measure the intensities of the protein bands [24].

2.9.Immunohistochemistry (IHC/IF)

Tumor tissues were harvested and embedded for cryosectioning. Serial sections (5 μm thickness) were prepared using a cryostat and mounted onto glass slides. The sections were fixed with 4% paraformaldehyde and subsequently blocked with 5% bovine serum albumin (BSA) to reduce non-specific binding. Sections were incubated overnight at 4°C with primary antibodies against ATP-binding cassette subfamily B member 1 (ABCB1), hypoxia-inducible factor-1 alpha (HIF-1α), and cleaved Caspase-3 (for all antibodies, 1:100). After washing, the sections were incubated with goat anti-rabbit secondary antibodies for 1 hour, conjugated with Alexa Fluor 488. Cell nuclei were counterstained with DAPI. Fluorescent images were acquired using a Cytation C10 confocal imaging system (BioTek) with a 20× objective at room temperature and processed using Gen5 software (BioTek). Quantitative analysis of fluorescence intensity was performed using Gen5 software by measuring average fluorescence intensity in representative regions of interest across experimental groups.

2.10. Enzyme-Linked Immunosorbent Assay (ELISA)

Tumor necrosis factor-α (TNF-α) levels in plasma and tumor tissues were quantified using commercially available ELISA kits (Sigma) according to the manufacturer's instructions. For tissue analysis, approximately 50 mg of freshly excised tumor tissue was homogenized in phosphate-buffered saline (PBS) to obtain a 10% (w/v) homogenate. Samples were centrifuged at 6000 rpm for 10 min, and the resulting supernatant was collected for analysis. TNF-α concentrations were determined by ELISA, and absorbance was measured according to the kit protocol. Protein concentration in tumor lysates and samples was determined using the Bradford assay and used for normalization where applicable [27].

2.11. Functional and pathway enrichment analysis

To contextualize the core hypoxia-associated markers examined in this study (HIF-1α, ABCB1, GLUT-1, BCL-2, Caspase-3) within their broader signaling networks, these targets were mapped onto KEGG (Kyoto Encyclopedia of Genes and Genomes) pathway annotations using SRplot, illustrating the extent of cross-talk between hypoxia, survival, metabolic, and apoptotic pathways rather than representing an unbiased, genome-wide enrichment analysis. Pathway enrichment visualization was performed using

the SRplot online platform (https://www.bioinformatics.com.cn/srplot), a free, web-based bioinformatics tool for data visualization and statistical analysis [28]. Pathways with $p < 0.05$ were considered statistically significant. Enriched pathways were grouped into functional categories, including Hypoxia signaling, general Signaling pathways (PI3K-Akt, MAPK, mTOR), Cell death (Apoptosis), Cancer-related pathways, Metabolism (central carbon metabolism in cancer, glycolysis/gluconeogenesis), Drug resistance (ABC transporters), and Cell cycle (p53 signaling pathway). Results were displayed as a bubble plot generated in SRplot, in which the x-axis represents the −log10(p-value), bubble size denotes the number of genes/proteins (count) associated with each pathway, and the color gradient indicates the level of statistical significance (ranging from green, −log10(p) ≈ 3.0, to red, −log10(p) ≈ 5.0). This enrichment analysis highlighted the HIF-1 signaling pathway, PI3K-Akt signaling pathway, and the broader "Pathways in cancer" category as the most significantly associated terms, consistent with the immunohistochemical findings for HIF-1α, P-glycoprotein/ABCB1, BCL-2, and GLUT-1, and supporting their involvement in hypoxia-driven tumor survival and chemoresistance.

2.12. Statistics

Statistical analyses of ICC/IF, RTCA, Western blot results, ELISA results, and rat body weight, tumor size, and tumor weight were performed using one-way ANOVA followed by Tukey's multiple comparisons test. IHC/IF data were analyzed using the Kruskal-Wallis test with Dunn's multiple comparisons test. Analyses were performed using GraphPad Prism 8 (San Diego, CA, USA), and $p < 0.05$ was considered statistically significant.

3. RESULTS

3.1. Moderate, but not severe, chemical hypoxia sensitizes breast cancer cells to chemotherapy-induced apoptosis

To recapitulate the hypoxic tumor microenvironment in vitro, SKBR3 and MDA-MB-231 cells were exposed to increasing concentrations of $CoCl_2$ (100–300 μM) in the sustained presence of TNF-α (10 ng/mL) (Figure 2). Immunocytochemical staining for HIF-1α confirmed successful induction of the hypoxic transcriptional program in both cell lines in a concentration-dependent manner. In SKBR3 cells, HIF-1α fluorescence intensity increased by approximately 2.8-fold at $CoCl_2$ 200 μM + TNF-α and by 3.1-fold at 300 μM + TNF-α relative to the DMSO control ($p < 0.0001$ for both, Figure 2, A and E). In MDA-MB-231 cells, comparable elevations of ~2.5-fold and ~3.0-fold were observed at 200 and 300 μM, respectively ($p < 0.001$, Figure 2, G and F). Critically, co-treatment with DOX (0.1 μM) and 5-FU (10 μM) did not significantly reduce HIF-1α expression in either cell line at any $CoCl_2$ concentration tested ($p > 0.05$ vs. corresponding hypoxia-only groups), indicating that the hypoxic transcriptional

response remained fully operative in the presence of cytotoxic agents. ABCB1 (P-glycoprotein/MDR1), a principal ATP-dependent drug efflux pump implicated in multidrug resistance, was significantly upregulated across all hypoxic conditions. In SKBR3, ABCB1 fluorescence intensity reached ~2.1-fold above control at $CoCl_2$ 100 μM + TNF-α and peaked at ~2.4-fold at 200 μM + TNF-α ($p < 0.01$). MDA-MB-231 cells exhibited a similar pattern, with ABCB1 expression rising to ~2.2-fold and ~2.6-fold at 100 and 200 μM + TNF-α, respectively ($p < 0.001$). Importantly, the addition of DOX/5-FU did not produce statistically significant downregulation of ABCB1 in either cell line at any hypoxic concentration ($p > 0.05$ vs. the corresponding Control groups), demonstrating that the drug resistance phenotype was not overcome by chemotherapy alone under hypoxic conditions. These findings suggest that ABCB1-mediated efflux activity remains competent within the chemical hypoxia model, potentially limiting intracellular drug accumulation. GLUT-1, the predominant facilitative glucose transporter transcriptionally regulated by HIF-1α, was substantially elevated in hypoxia-only groups. In SKBR3, GLUT-1 intensity reached ~1.7-fold, ~3.8-fold, and ~2.9-fold above control at $CoCl_2$ 100, 200, and 300 μM + TNF-α, respectively ($p < 0.0001$ at 200 μM). However, co-treatment with DOX/5-FU produced a marked and statistically significant reduction in GLUT-1 expression specifically at the 200 μM $CoCl_2$ condition, decreasing intensity to approximately ~1.1-fold above control — representing a reduction of approximately 71% relative to the hypoxia-only 200 μM group ($p < 0.0001$). An analogous, though less pronounced, reduction was observed in MDA-MB-231 cells, where GLUT-1 decreased by ~58% in the 200 μM CT+DF group compared to the corresponding hypoxia-only condition ($p < 0.001$). This selective suppression of glucose uptake capacity under mild hypoxia combined with chemotherapy suggests enhanced metabolic vulnerability of cancer cells, potentially amplifying cytotoxic efficacy. Caspase-3, the principal executioner cysteine protease of the intrinsic and extrinsic apoptotic pathways, was used as a functional readout of chemotherapy-induced cell death. In SKBR3 cells, Caspase-3 fluorescence intensity was modestly elevated in hypoxia-only groups (100 μM: ~1.3-fold; 200 μM: ~1.6-fold; $p < 0.05$). Upon addition of DOX (0.1 μM) and 5-FU (10 μM), a significant and concentration-dependent potentiation of Caspase-3 activation was observed, peaking in the $CoCl_2$ 100 μM + TNF-α + DOX/5-FU and 200 μM + TNF-α + DOX/5-FU groups, reaching approximately ~3.2-fold and ~3.8-fold above control, respectively ($p < 0.001$ and $p < 0.0001$). Notably, the 300 μM + TNF-α + DOX/5-FU group exhibited significantly attenuated Caspase-3 cleavage (~1.2-fold above control), which was not statistically different from the DMSO control ($p > 0.05$; ns), suggesting that severe chemical hypoxia paradoxically confers protection against apoptosis in SKBR3 cells. In MDA-MB-231 cells, a distinct pattern was observed. Both the 200 μM and 300 μM + TNF-α + DOX/5-FU groups displayed robust Caspase-3 upregulation, reaching approximately ~2.6-fold and ~2.9-fold above control, respectively ($p < 0.001$ and $p < 0.001$), indicating that MDA-MB-231 cells maintain chemosensitivity across a broader hypoxic range. These data collectively demonstrate that mild-to-moderate chemical hypoxia, most

339 effectively achieved with $CoCl_2$ at 200 μM, creates an intracellular context that sensitizes breast cancer
340 cells — irrespective of receptor subtype — to DOX/5-FU-induced apoptotic signaling, as evidenced by
341 maximal induction of Caspase-3 cleavage.

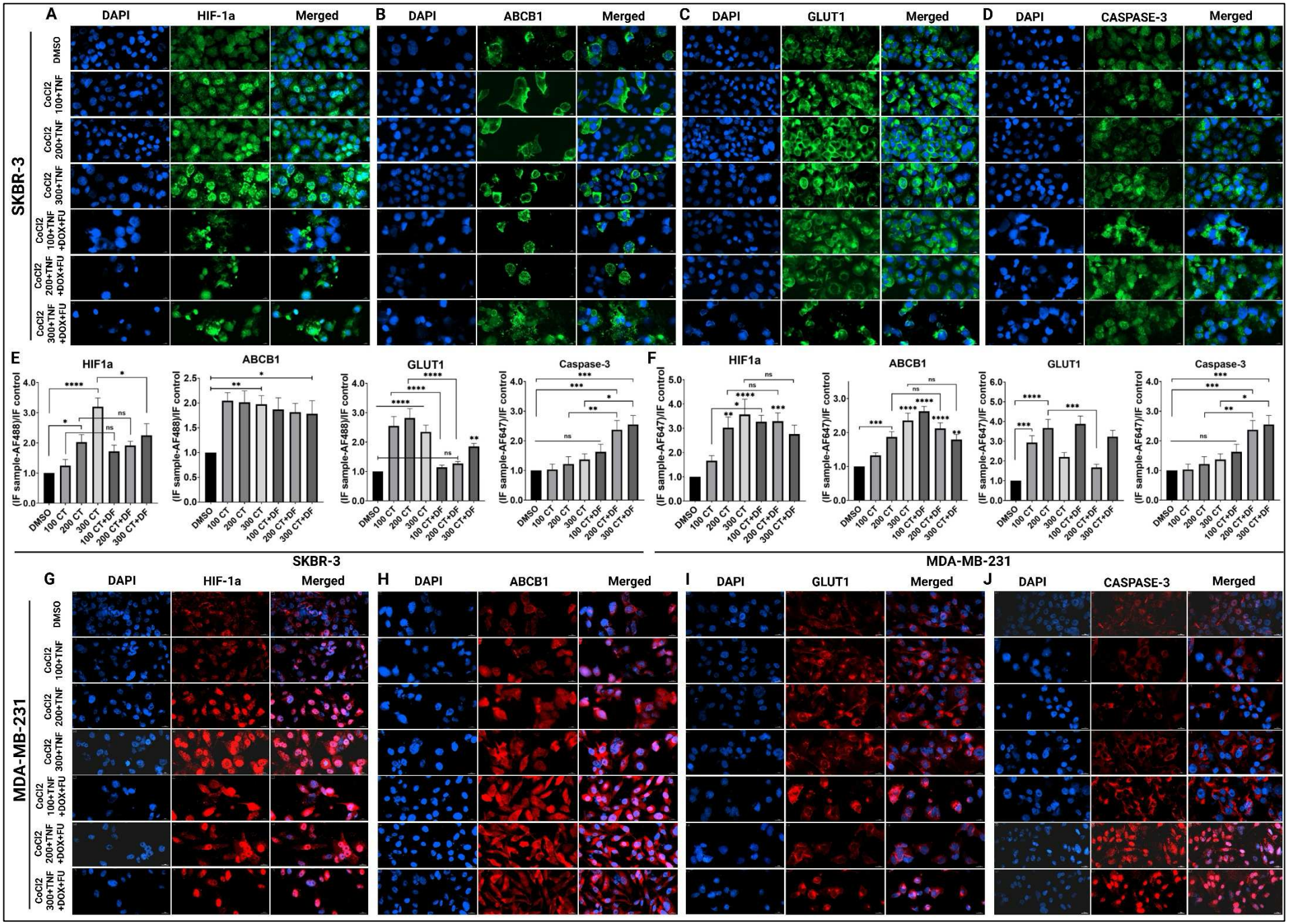

A
DAPI
HIF-1a
Merged
B
DAPI
ABCB1
Merged
C
DAPI
GLUT1
Merged
D
DAPI
CASPASE-3
Merged
SKBR-3
DMSO
CoCl2 100+TNF
CoCl2 200+TNF
CoCl2 300+TNF
CoCl2 100+TNF +DOX+FU
CoCl2 200+TNF +DOX+FU
CoCl2 300+TNF +DOX+FU
E
HIF1a
ABCB1
GLUT1
Caspase-3
(IF sample-AF488)/IF control
F
(IF sample-AF647)/IF control
DMSO
100 CT
200 CT
300 CT
100 CT+DF
200 CT+DF
300 CT+DF
SKBR-3
MDA-MB-231
G
H
I
J

Figure 2. Immunocytochemical analysis of HIF-1α, ABCB1, GLUT-1, and Caspase-3 expression in SKBR3 and MDA-MB-231 breast cancer cell lines under chemical hypoxia and combination chemotherapy. SKBR3 (HER2-enriched; panels A–D) and MDA-MB-231 (triple-negative; panels G–J) cells were treated with cobalt chloride ($CoCl_2$; 100, 200, or 300 μM) in combination with recombinant human TNF-α (10 ng/mL) to induce chemical hypoxia mimicking the tumor microenvironment, with or without concurrent doxorubicin (DOX; 0.1μM) and 5-fluorouracil (5-FU; 10 μM) co-treatment. DMSO-treated cells served as the vehicle control. Following treatment, cells were fixed, permeabilized, and incubated with primary antibodies against HIF-1α, ABCB1, GLUT-1, and Caspase-3 (all diluted 1:250), followed by species-appropriate secondary antibodies conjugated to Alexa Fluor 488 (AF488; SKBR3, green) or Alexa Fluor 647 (AF647; MDA-MB-231, red). Nuclei were counterstained with DAPI (blue). Fluorescence imaging was performed using a Cytation C10 Confocal Multi-Mode Reader at ×20 magnification with a 10 μm scale reference. Panels E and F present quantitative fluorescence intensity ratios (IF sample / IF control) for SKBR3 and MDA-MB-231, respectively, expressed relative to the DMSO control (set to 1.0). Data represent the mean ± SEM from three independent experiments performed in triplicate. Statistical significance was determined by one-way ANOVA followed by Tukey's post-hoc test: *p < 0.05, **p < 0.01, ***p < 0.001, ****p < 0.0001; ns, not significant. CT, $CoCl_2$ + TNF-α; DF, DOX + 5-FU.

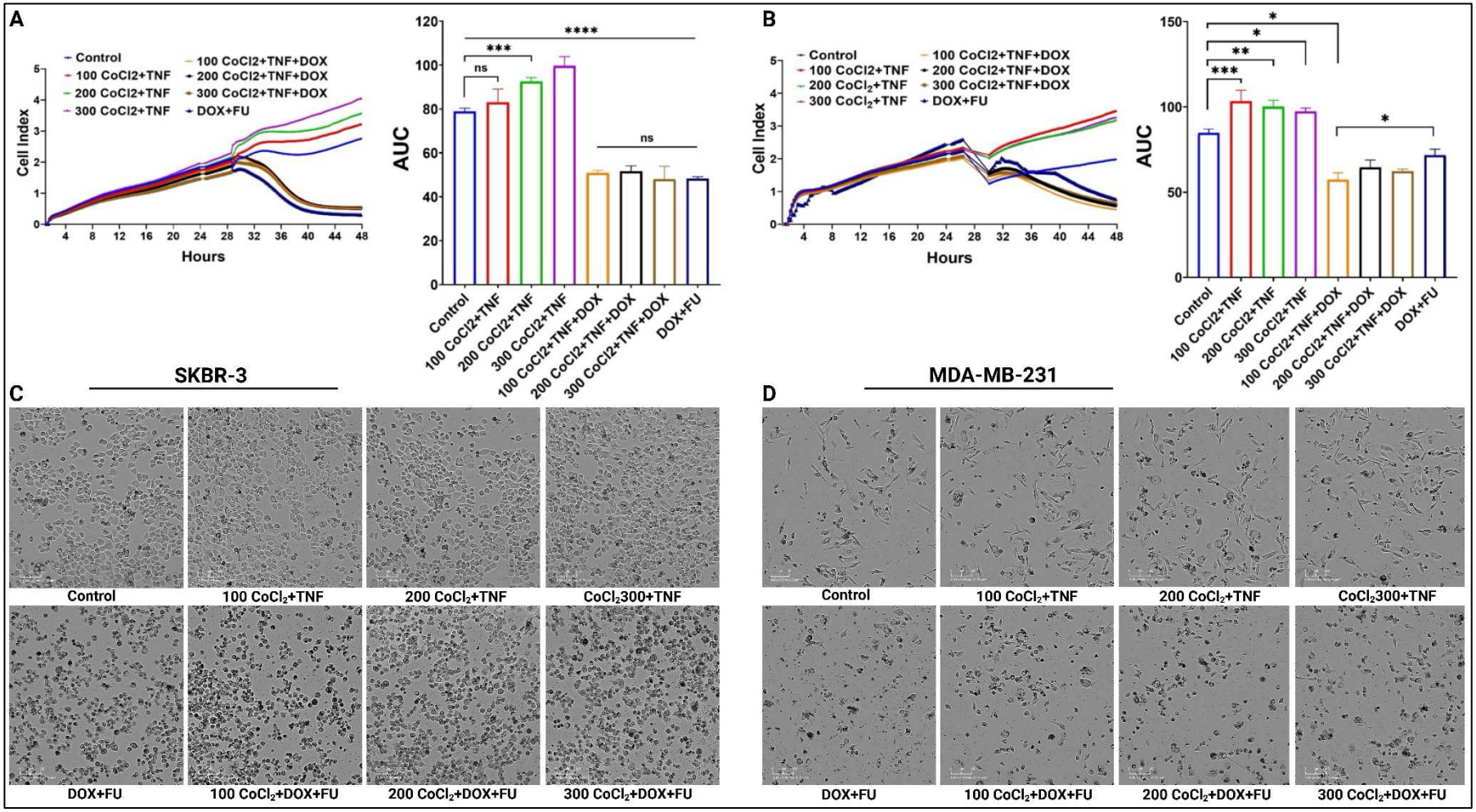


Figure 3. Real-time monitoring of $CoCl_2$/TNF-α-induced hypoxia and FUDOX chemosensitivity in SKBR-3 and MDA-MB-231 breast cancer cell lines using the xCELLigence RTCA eSight system. SKBR-3 (20,000 cells/well) and MDA-MB-231 (10,000 cells/well) cells were monitored continuously for 48 h. (A, B) Real-time cell index profiles for SKBR-3 and MDA-MB-231, respectively, showing proliferation kinetics under the indicated conditions: untreated control; chemical hypoxia induced by $CoCl_2$ (100, 200, or 300 µM) combined with TNF-α (10 ng/mL); $CoCl_2$ (100, 200, or 300 µM) combined with TNF-α and subsequent FUDOX chemotherapy; and FUDOX alone. Corresponding AUC quantification is shown to the right of each cell index plot, presented as mean ± SD (n = 4 for SKBR-3 and MDA-MB-231); ns, not significant; *p < 0.05; **p < 0.01; ***p < 0.001; ****p < 0.0001 (one-way ANOVA with Tukey's multiple comparisons test). (C, D) Representative phase-contrast images (eSight imaging module, ×10 objective, scale bar = 100 µm) acquired at the experimental endpoint for SKBR-3 (C) and MDA-MB-231 (D), illustrating morphological changes and cell density corresponding to each treatment condition.

3.2. Hypoxic preconditioning does not confer resistance to FUDOX cytotoxicity in real time

To evaluate whether hypoxia-mimetic conditioning alters chemosensitivity to FUDOX (5-fluorouracil + doxorubicin), we performed real-time cell analysis (RTCA) on SKBR-3 and MDA-MB-231 breast cancer cells using the xCELLigence eSight platform. All treatment groups exhibited comparable proliferation kinetics during the initial ~28 h baseline period, confirming uniform seeding and growth before intervention (Figure 3, A, B).

In SKBR-3 cells, exposure to $CoCl_2$ combined with TNF-α produced a dose-dependent increase in cell index and AUC relative to control, reaching statistical significance at 200 μM ($p < 0.001$) and 300 μM ($p < 0.0001$), while the 100 μM dose did not differ significantly from control (ns) (Figure 3A). Subsequent FUDOX treatment, whether preceded by hypoxic conditioning or administered alone, induced a marked decline in cell index beginning shortly after drug addition, with no significant differences in AUC among the four FUDOX-containing groups (ns), indicating that prior $CoCl_2$-induced hypoxia did not modulate the cytotoxic response to FUDOX in this cell line.

A similar pattern was observed in MDA-MB-231 cells, where $CoCl_2$+TNF-α treatment significantly increased AUC relative to control at all three concentrations tested (100 μM, $p < 0.001$; 200 μM, $p < 0.01$; 300 μM, $p < 0.05$) (Figure 3B). FUDOX treatment again produced a pronounced reduction in cell index across all groups; notably, the FUDOX-alone group showed a modest but statistically significant increase in AUC compared with the $CoCl_2$+TNF-α+FUDOX combination groups ($p < 0.05$), suggesting a subtle influence of hypoxic preconditioning on the overall chemotherapeutic response curve in MDA-MB-231 cells, despite the absence of a clear morphological rescue effect.

Consistent with the impedance-based data, representative endpoint phase-contrast images (Figure 3, C, D) showed that control and $CoCl_2$+TNF-α-treated wells retained high cell density with typical adherent morphology in both cell lines, whereas all FUDOX-containing groups exhibited pronounced loss of cell density, rounding, and detachment characteristic of cytotoxic cell death, irrespective of prior hypoxic conditioning.

3.3.FUDOX suppresses tumor growth and improves survival independent of oxygenation status

To validate the in vitro findings in a physiologically relevant setting, we next evaluated the effects of intermittent hypoxia and chemotherapy in an in vivo breast cancer model (Figure 1 and 4). At the end of the experimental period, all tumors were excised and measured following euthanasia of the animals.

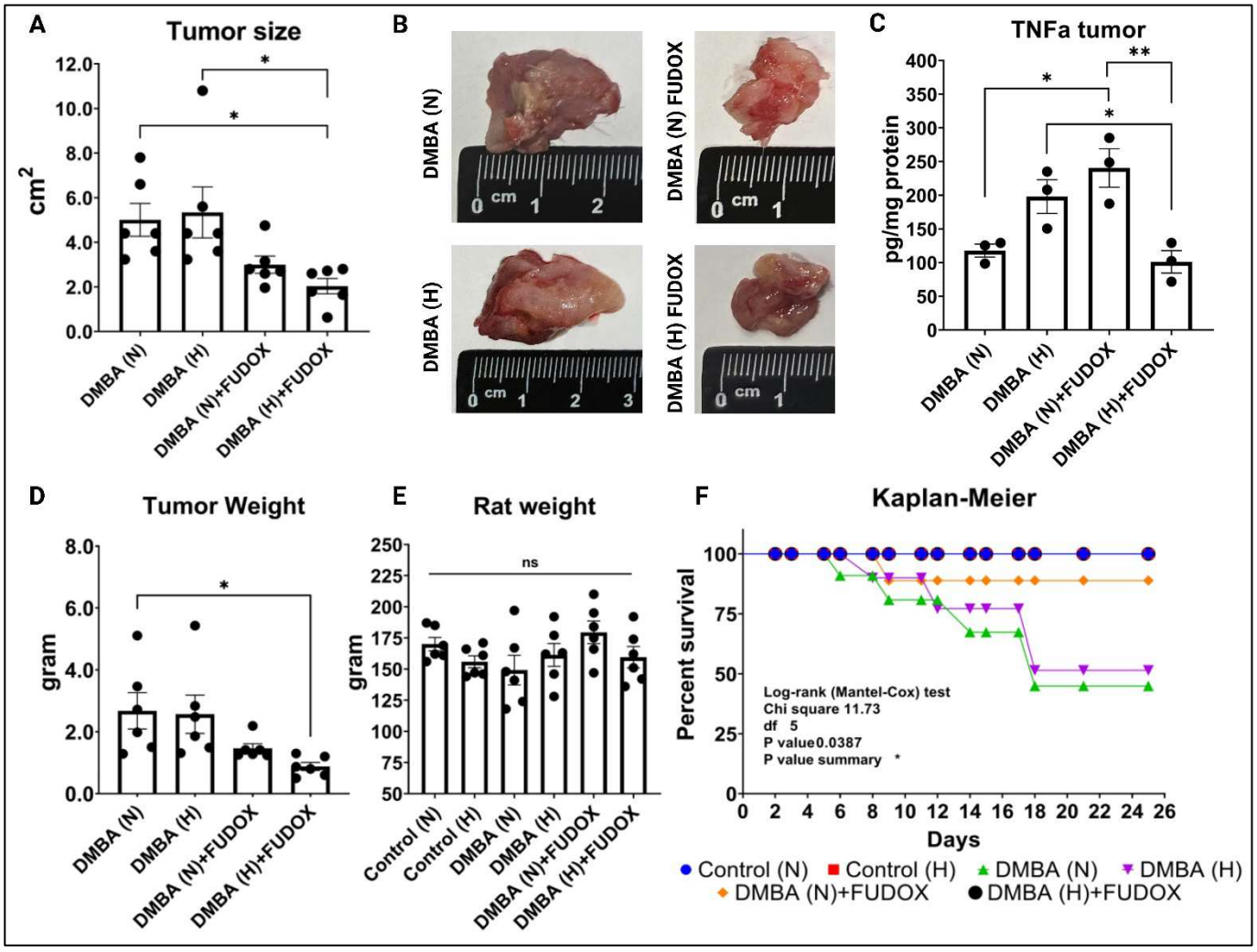


Figure 4. Combined 5-FU and doxorubicin (FUDOX) treatment reduces tumor burden and improves survival in DMBA-induced mammary carcinogenesis under normoxic and hypoxic conditions. (A) Tumor size (cm²) in DMBA-induced tumors under normoxic (N) and hypoxic (H) conditions, with or without FUDOX treatment. Both FUDOX-treated groups showed significantly reduced tumor size compared to untreated DMBA controls (*p < 0.05). (B) Representative gross morphology of excised mammary tumors from DMBA(N), DMBA(N)+FUDOX, DMBA(H), and DMBA(H)+FUDOX groups; ruler scale (cm) provided for size reference. (C) Tumor tissue TNF-α concentrations (pg/mL), determined by ELISA, across the six experimental groups. (D) Tumor weight (g) was significantly reduced in the DMBA(H)+FUDOX group compared to untreated DMBA(N) controls (*p < 0.05). (E) Rat body weight (g) at endpoint showed no significant differences across the six experimental groups (ns), indicating that FUDOX treatment did not cause systemic toxicity. (F) Kaplan-Meier survival curves for all six groups (Control N, Control H, DMBA N, DMBA H, DMBA(N)+FUDOX, DMBA(H)+FUDOX) over a 26-day observation period. Log-rank (Mantel-Cox) test indicated a statistically significant difference in survival probability among groups ($\chi^2 = 11.73$, df = 5, p = 0.0387). Data in (A), (C), (D), and (E) are expressed as mean ± SEM, with individual data points representing single animals.

To evaluate the therapeutic efficacy of combined 5-fluorouracil and doxorubicin (FUDOX) treatment on DMBA-induced mammary carcinogenesis, tumor size, weight, and animal survival were assessed under both normoxic and hypoxic conditions (Figure 4). FUDOX treatment markedly reduced tumor size in both normoxic and hypoxic groups compared to their respective untreated DMBA controls (Figure 4, A, $p < 0.05$ for DMBA (H)+FUDOX vs DMBA), with the most pronounced reduction observed in the DMBA(H)+FUDOX group (mean tumor size approximately 2.0 cm^2, versus 5.0–5.3 cm^2 in untreated DMBA(N) and DMBA(H) groups). Gross morphological examination of excised tumors confirmed this reduction, with FUDOX-treated tumors appearing visibly smaller and more compact than untreated controls (Figure 4, B).

Tumor TNF-α concentrations differed according to oxygenation status (Figure 4, C). Intermittent hypoxia significantly increased TNF-α levels compared with normoxic DMBA tumors ($p < 0.05$). Under normoxic conditions, FUDOX treatment resulted in a significant increase in TNF-α compared with untreated DMBA tumors ($p < 0.05$). In contrast, under hypoxic conditions, FUDOX significantly reduced TNF-α levels relative to the untreated DMBA(H) group ($p < 0.05$). Consequently, TNF-α concentrations in the DMBA(H)+FUDOX group were approximately 2.5-fold lower than those in the untreated hypoxic DMBA group ($p < 0.01$).

Consistent with the tumor size data, tumor weight was significantly lower in the DMBA(H)+FUDOX group relative to untreated DMBA(N) controls (Figure 4, D, $p < 0.05$), supporting the antitumor efficacy of the combined treatment regimen. Importantly, body weight measurements at the experimental endpoint showed no significant differences among any of the six groups (Figure 4, E, ns), suggesting that FUDOX administration was well tolerated and did not result in systemic toxicity or treatment-related weight loss.

Survival analysis further demonstrated the therapeutic benefit of FUDOX treatment (Figure 4, F). Kaplan-Meier curves revealed that both FUDOX-treated groups maintained substantially higher survival rates over the 26-day observation period compared to untreated DMBA controls, which exhibited survival declines beginning around day 8–10 and reaching approximately 45–50% by the end of the study (Figure 4, F). Control animals (both normoxic and hypoxic, untreated) maintained 100% survival throughout the observation period. The log-rank (Mantel-Cox) test confirmed a statistically significant difference in survival distribution among the six groups ($\chi^2 = 11.73$, $df = 5$, $p = 0.0387$), indicating that FUDOX treatment conferred a significant survival advantage in DMBA-induced tumor-bearing rats regardless of oxygenation status.

3.4.FUDOX attenuates hypoxia-driven HIF-1α/ABCB1 signaling and restores apoptotic capacity in vivo

As shown in Figure 5, IHC-IF, immunofluorescence analysis of tumor sections, revealed a pattern consistent with the western blot findings for HIF-1α and P-gp/ABCB1. In the DMBA+hypoxia group, both HIF-1α and P-gp/ABCB1 immunoreactivity were increased relative to the DMBA control group, whereas no appreciable change was observed in the DMBA+5FU+DOX group compared with DMBA (Figure 5). In the DMBA+5FU+DOX+hypoxia group, HIF-1α and P-gp/ABCB1 signals were reduced compared with the DMBA+hypoxia group, but remained higher than those in the DMBA and DMBA+5FU+DOX groups. Caspase-3 showed a distinct pattern (Figure 5, B). No marked increase in caspase-3 immunoreactivity was observed in the DMBA+hypoxia group compared with DMBA, indicating that hypoxia alone did not activate a detectable apoptotic response in the tumor tissue (Figure 5, B and D). In contrast, Caspase-3 staining increased in the DMBA+5FU+DOX group relative to DMBA and was further markedly enhanced in the DMBA+5FU+DOX+hypoxia group, suggesting that combined hypoxia and chemotherapy induced the strongest caspase-3-associated apoptotic signal among the experimental groups.

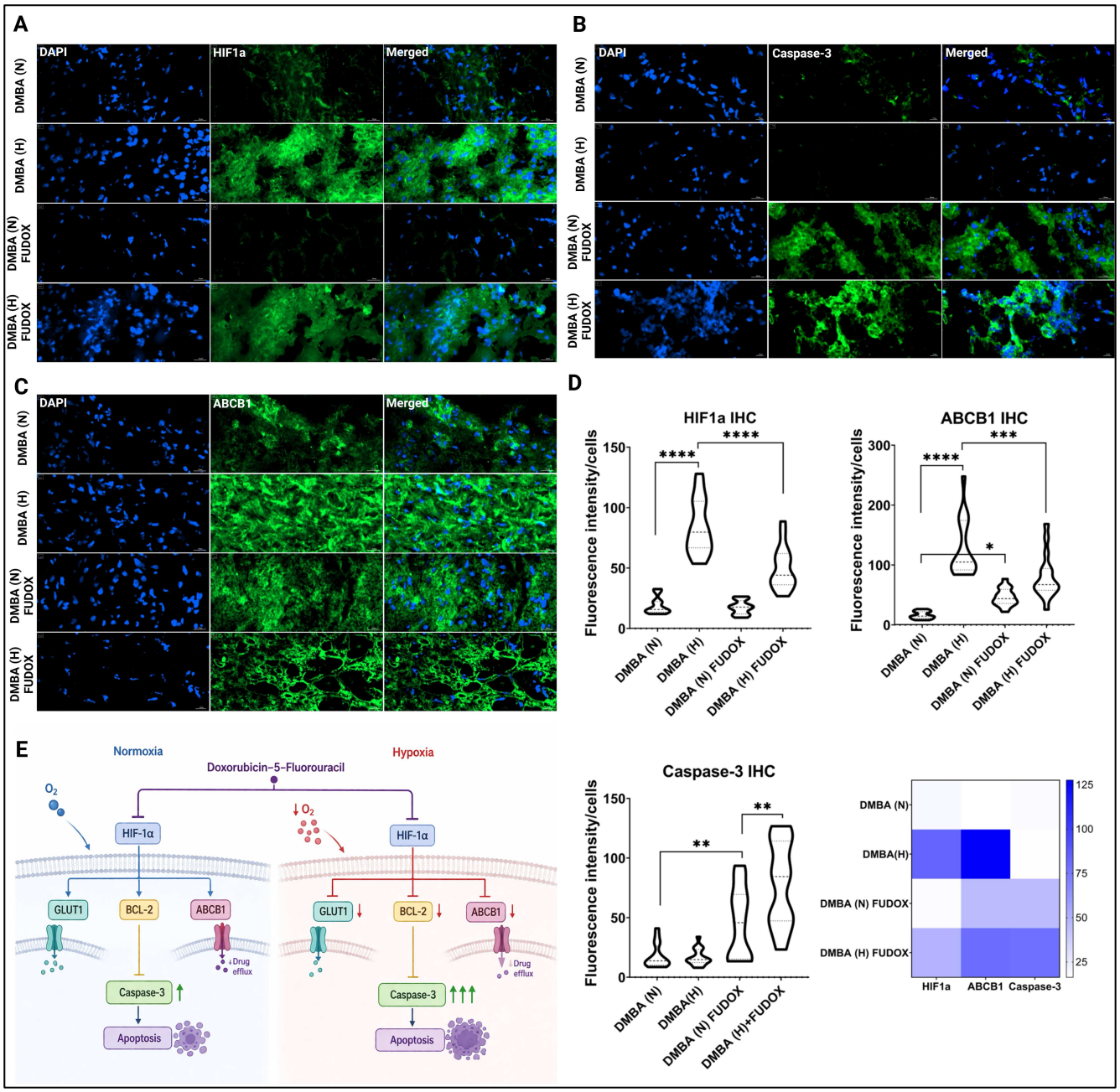


Figure 5. 5-FU+DOX (FUDOX) suppresses hypoxia-induced tumor progression by modulating HIF-1α signaling, ABCB1 expression, and apoptotic pathways. (A–C) Representative immunofluorescence images showing the expression of HIF-1α (A), cleaved Caspase-3 (B), and ABCB1 (C) in experimental groups. Nuclei were counterstained with DAPI (blue), while target proteins are shown in green. Merged images demonstrate the localization and relative abundance of each marker. Under hypoxic conditions, HIF-1α and ABCB1 expression were markedly elevated, whereas Caspase-3 staining was reduced. Treatment with FUDOX attenuated hypoxia-induced HIF-1α and ABCB1 upregulation and restored apoptotic signaling, as evidenced by increased Caspase-3 immunoreactivity. (D) Quantitative analysis of immunofluorescence intensity per cell for HIF-1α, ABCB1, and Caspase-3. Violin plots represent the distribution of fluorescence intensities obtained from individual cells across experimental groups. Statistical significance was determined using one-way ANOVA followed by appropriate multiple-comparison testing. Data are presented as the median with interquartile distribution. *P < 0.05, **P < 0.01, ***P < 0.001, ****P < 0.0001. Correlation heatmap depicting the relationships among HIF-1α, ABCB1, and Caspase-3 expression levels. Positive correlations were observed between HIF-1α and ABCB1, whereas Caspase-3 showed an inverse association with both markers, supporting the proposed mechanism

of FUDOX-mediated regulation of hypoxia-associated tumor adaptation. (E) Proposed mechanistic model illustrating the effects of FUDOX under normoxic and hypoxic conditions. Under normoxia, HIF-1α undergoes hydroxylation-mediated degradation, maintaining low ABCB1 expression and limiting tumor progression. Hypoxia stabilizes HIF-1α, leading to enhanced transcription of ABCB1 and suppression of apoptotic signaling, thereby promoting cancer cell survival. FUDOX counteracts hypoxia-driven responses by reducing HIF-1α stabilization, downregulating ABCB1 expression, and activating Caspase-3-dependent apoptosis, ultimately suppressing tumor progression.

3.5.Hypoxia-driven survival and resistance markers are partially reversed by FUDOX treatment in vivo

As shown in Figure 6, Western blot analysis of tumor tissues demonstrated a marked hypoxia-associated increase in HIF-1α, P-gp/ABCB1, and BCL-2 expression in the DMBA+hypoxia group compared with the DMBA control group. HIF-1α levels increased approximately fourfold following intermittent mild hypoxia, indicating robust activation of the hypoxic response within the tumor microenvironment (Figure 6, A, B, and C). A similar upward trend was observed for P-gp/ABCB1 and BCL-2 in the DMBA+hypoxia group. In contrast, treatment with 5-fluorouracil and doxorubicin alone did not produce a discernible change in the expression of these proteins relative to the DMBA group. In the DMBA+5FU+DOX+hypoxia group, HIF-1α, P-gp/ABCB1, and BCL-2 were reduced relative to the DMBA+hypoxia group, although their expression remained higher than in the DMBA and DMBA+5FU+DOX groups. GLUT-1 exhibited a distinct pattern: its expression was slightly elevated in the DMBA+hypoxia group, remained comparable to the DMBA group in the DMBA+5FU+DOX group, and was most strongly reduced in the DMBA+5FU+DOX+hypoxia group, where it was lower than in all other experimental groups (Figure 6, A, B, and C).

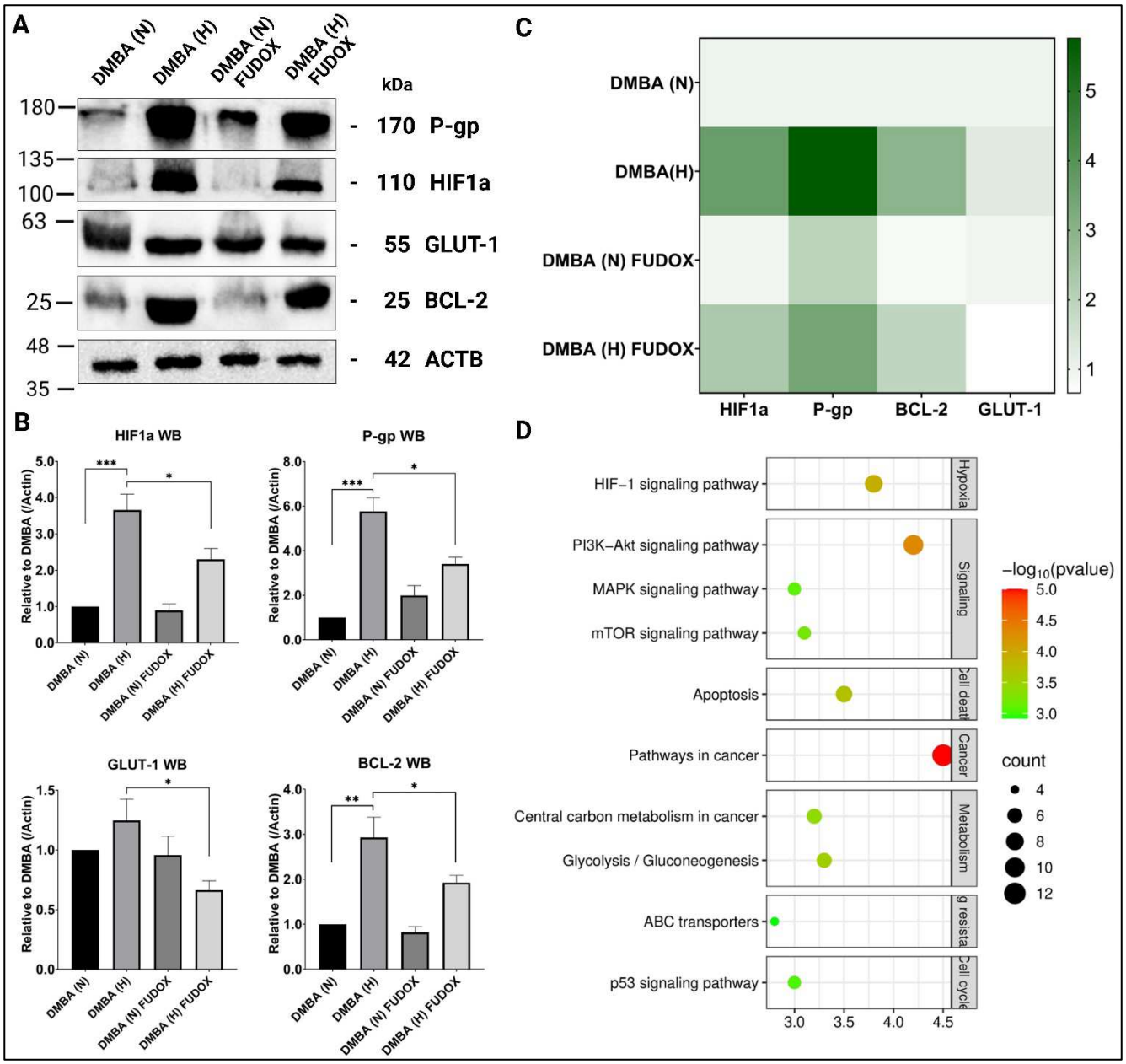


Figure 6. Hypoxia promotes the expression of HIF-1α-associated survival and drug-resistance markers, while FUDOX treatment partially reverses these effects in DMBA-induced tumors. (A) Representative Western blot analysis of P-glycoprotein (P-gp/ABCB1), HIF-1α, GLUT-1, and BCL-2 protein expression in tumors from the experimental groups: DMBA under normoxic conditions [DMBA (N)], DMBA under hypoxic conditions [DMBA (H)], DMBA treated with FUDOX under normoxia [DMBA (N)+FUDOX], and DMBA treated with FUDOX under hypoxia [DMBA (H)+FUDOX]. β-Actin was used as the loading control. (B) Densitometric quantification of Western blot data normalized to β-actin. Hypoxia significantly increased the expression of HIF-1α, P-gp, GLUT-1, and BCL-2 compared with normoxic controls. FUDOX treatment reduced the hypoxia-induced upregulation of these proteins, indicating attenuation of hypoxia-associated metabolic adaptation, chemoresistance, and pro-survival signaling. Data are presented as mean ± SEM. Statistical significance is indicated as *P < 0.05, **P < 0.01, ***P < 0.001. (C) Heatmap

(GraphPad Prism) visualization of relative protein expression levels across experimental groups. Increased expression of HIF-1α, P-gp, and BCL-2 was observed in the hypoxic DMBA group, whereas FUDOX treatment reduced their expression. Color intensity corresponds to normalized protein abundance. (D) Functional enrichment analysis of differentially expressed proteins and associated signaling pathways. The identified molecular alterations were enriched in pathways related to HIF-1 signaling, PI3K–Akt signaling, MAPK signaling, mTOR signaling, apoptosis, ABC transporter regulation, glycolysis/gluconeogenesis, central carbon metabolism in cancer, p53 signaling, and broader cancer-associated pathways, highlighting the central role of hypoxia-driven signaling networks in tumor progression and therapeutic response.

Overall, the combined western blot and immunofluorescence findings indicate that mild intermittent hypoxia substantially modified the tumor phenotype. In both assays, hypoxia alone was associated with increased HIF-1α and P-gp/ABCB1 expression, together with elevated BCL-2 and no evident increase in caspase-3, suggesting activation of a hypoxia-adaptive, pro-survival program. In contrast, 5FU+DOX treatment alone produced little or no change in HIF-1α, P-gp/ABCB1, or BCL-2, indicating a limited effect on these resistance-associated markers under the present conditions. When chemotherapy was combined with hypoxia, HIF-1α, P-gp/ABCB1, and BCL-2 remained lower than in the hypoxia-only group but did not return to control levels, whereas caspase-3 was markedly increased, particularly in the immunofluorescence analysis. Taken together, these results suggest that mild intermittent hypoxia promotes a tumor survival and chemoresistance-associated phenotype. In contrast, the addition of 5FU+DOX is associated with partial suppression of the hypoxia-driven response and a stronger apoptotic signal. This pattern supports a context-dependent effect of hypoxia on tumor biology: hypoxia alone appears to favor adaptation and survival, whereas in the presence of chemotherapy, it is associated with enhanced caspase-3-mediated apoptosis. To contextualize these protein-level findings within broader signaling networks, differentially expressed proteins were subjected to KEGG pathway enrichment analysis (Figure 6, D). The most significantly enriched pathways included HIF-1 signaling, PI3K–Akt signaling, MAPK signaling, mTOR signaling, apoptosis, ABC transporter regulation, glycolysis/gluconeogenesis, central carbon metabolism in cancer, and p53 signaling, indicating that the hypoxia-associated proteins identified in this study (HIF-1α, P-gp/ABCB1, GLUT-1, BCL-2, and Caspase-3) converge on a coordinated network of survival, metabolic, and apoptotic signaling pathways rather than acting through isolated, independent mechanisms. This pathway-level convergence reinforces the interpretation that intermittent hypoxia engages a systems-level adaptive response in DMBA-induced tumors, which is only partially uncoupled by FUDOX treatment.

4. DISCUSSION

The present study sought to determine whether mild, intermittent oxygen fluctuation—rather than the chronic, severe hypoxia traditionally associated with tumor progression—could redirect breast cancer cells toward a more chemotherapy-responsive phenotype (Figure 7). Across complementary in vitro and in vivo models, our results converge on a consistent and somewhat counterintuitive conclusion: hypoxia per se reinforced a survival-oriented, treatment-resistant transcriptional program, yet its combination with cytotoxic chemotherapy produced the strongest pro-apoptotic and tumor-suppressive outcomes observed in either model. This pattern is most parsimoniously interpreted within the conceptual framework of hormesis, wherein a sub-lethal stressor—here, controlled oxygen deprivation—does not simply potentiate the underlying pathology but instead recalibrates cellular stress-response circuitry in a manner that can favor a subsequent insult, namely chemotherapy-induced cytotoxic stress [29,30].

Hypoxia and inflammation reinforce a canonical survival program. Both the in vitro chemical hypoxia/inflammation model ($CoCl_2$/TNF-α) and the in vivo intermittent hypoxia protocol reproduced the expected hallmarks of HIF-1α pathway activation: concentration- and exposure-dependent induction of HIF-1α itself, together with upregulation of its downstream effectors ABCB1/P-glycoprotein and, in tumor tissue, BCL-2. This is entirely consistent with the well-established role of HIF-1α as the master transcriptional regulator of the hypoxic adaptive response, coordinating glycolytic reprogramming, anti-apoptotic signaling, and multidrug efflux capacity [7,31]. The persistence of elevated ABCB1 expression even in the presence of doxorubicin and 5-fluorouracil is particularly notable, as ABCB1-mediated efflux is among the best-characterized mechanisms by which HIF-1α confers chemoresistance, having been demonstrated to limit intracellular accumulation of anthracyclines and other substrates across multiple tumor types [32,33]. That this resistance axis remained intact under combination treatment in our model indicates that chemosensitization, where observed, did not occur through suppression of drug efflux capacity, but rather through mechanisms acting downstream of, or in parallel to, the canonical resistance pathway.

A biphasic, concentration-dependent relationship between hypoxic severity and chemosensitivity was observed. The most striking in vitro finding was the non-monotonic relationship between $CoCl_2$ concentration and caspase-3 activation following DOX/5-FU co-treatment. Moderate chemical hypoxia (200 μM) maximized executioner caspase-3 induction in both SKBR3 and MDA-MB-231 cells, whereas severe hypoxia (300 μM) blunted this apoptotic response in SKBR3 cells toward baseline. This is consistent with the principle, increasingly recognized across hormesis and preconditioning literature, that the biological consequence of a stressor is critically dependent on its intensity, duration, and pattern rather than being a simple linear function of stressor severity [5,7,30]. Under conditions of mild-to-moderate hypoxic stress, transient increases in reactive oxygen species and metabolic perturbation may

prime apoptotic machinery without triggering the compensatory, fully protective adaptive program that emerges under more severe or prolonged hypoxic insult [34,35]. The selective, hypoxia-dependent suppression of GLUT-1 observed specifically at 200 µM $CoCl_2$ in combination with DOX/5-FU offers one plausible mechanistic thread: by constraining glycolytic flux precisely at the hypoxic threshold that otherwise demands maximal glucose dependency, chemotherapy co-treatment may impose a metabolic vulnerability that tips the balance from adaptive survival toward apoptotic commitment [36,37]. This interpretation aligns with broader evidence that glycolytic inhibition can sensitize tumor cells to chemotherapeutic agents, particularly in glycolysis-dependent breast cancer subtypes [38].

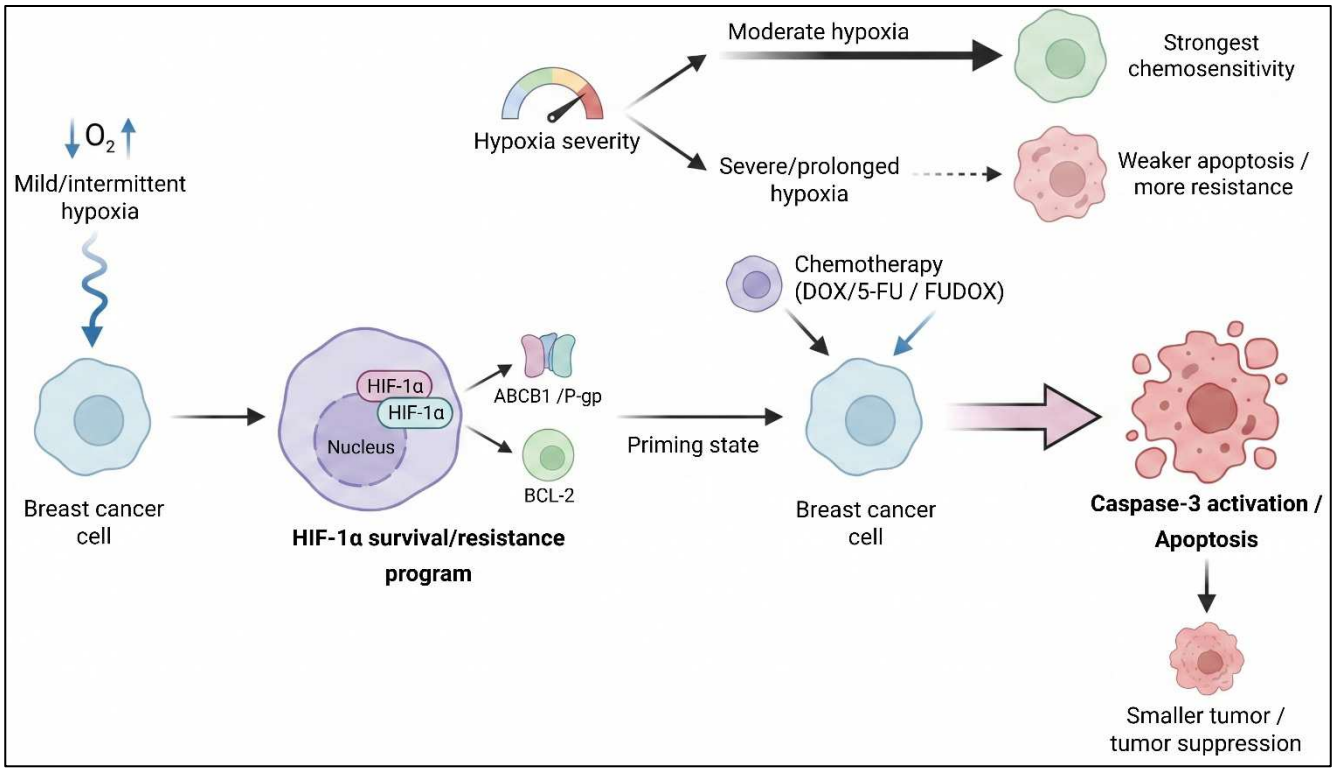


Figure 7. Proposed mechanistic model of the biphasic hypoxia–chemosensitivity relationship in breast cancer cells. Mild/intermittent hypoxia (↓O_2) activates a HIF-1α–driven survival/resistance program in breast cancer cells, upregulating the drug efflux transporter ABCB1/P-glycoprotein and the anti-apoptotic protein BCL-2. Rather than conferring protection, this HIF-1α-dependent adaptive state places cells into a "priming" condition that enhances their subsequent responsiveness to chemotherapy (DOX/5-FU/FUDOX). The severity and duration of hypoxia determine the direction of this effect: moderate, intermittent hypoxic stress yields the strongest chemosensitivity, driving robust caspase-3 activation, apoptosis, and tumor suppression upon chemotherapy exposure, whereas severe or prolonged hypoxia shifts the balance toward weaker apoptotic responses and greater chemoresistance. This model reconciles the classical view of hypoxia as a driver of chemoresistance with the present findings, in which mild oxygen fluctuation sensitizes rather than protects breast cancer cells, despite concurrent HIF-1α/ABCB1 upregulation.

Translation to the in vivo tumor microenvironment. The in vivo findings reproduced this pattern at a systemic level. Intermittent mild hypoxia alone increased tumor burden and tumor-associated HIF-1α, P-glycoprotein/ABCB1, and BCL-2 expression—an outcome consistent with hypoxia's established tumor-promoting and chemoresistance-conferring role in vivo [39]. Yet when intermittent hypoxia was combined with FUDOX chemotherapy, tumors were smaller than in either the hypoxia-only or chemotherapy-only groups, body weight was unaffected, and survival was significantly improved relative to untreated controls. The concurrent rise in caspase-3 immunoreactivity—absent in the hypoxia-only condition but markedly amplified specifically in the combination group—mirrors the in vitro biphasic relationship. It suggests that the same hormetic principle operates within the intact tumor microenvironment, not merely in isolated cell culture. The concordance between our in vitro chemical hypoxia model, in which TNF-α was exogenously supplied to mimic the inflammatory tumor microenvironment, and the elevated plasma/tumor TNF-α levels observed under intermittent hypoxia in vivo (Figure 4, C) supports a physiologically relevant crosstalk between hypoxic and inflammatory signaling in this model. Hypoxia and TNF-α/NF-κB signaling are known to reinforce one another: NF-κB activation downstream of TNF-α can transcriptionally upregulate HIF-1α, while HIF-1α, in turn, can amplify inflammatory cytokine production, creating a self-sustaining hypoxia-inflammation loop that promotes tumor cell survival and drug resistance [22,40]. Our finding that this loop remained active despite FUDOX treatment further underscores the resilience of the hypoxia-associated pro-survival program, even as apoptotic signaling was concurrently potentiated. This pathway-mapping exercise underscores a broader translational challenge: the interconnected, multi-pathway nature of hypoxia-driven signaling makes it inherently difficult to extrapolate single-pathway in vitro perturbations to the full complexity of an in vivo tumor, where compensatory and cross-regulatory mechanisms remain incompletely defined.

A working hypoxic-conditioning model. Taken together, these findings support a working model in which controlled, intermittent hypoxic exposure exerts dual and temporally separable effects: it sustains canonical hypoxia-adaptive signaling (HIF-1α, ABCB1, BCL-2) that would, in isolation, favor tumor survival and progression, while simultaneously establishing a metabolically and apoptotically primed cellular state that becomes selectively unmasked—and therapeutically exploitable—only in the presence of cytotoxic chemotherapy. This is conceptually distinct from classical hypoxia-driven chemoresistance models, which assume a monotonic relationship between hypoxic severity and treatment failure. Our data instead suggest a threshold phenomenon, consistent with hormetic dose-response frameworks described in other pathophysiological contexts such as ischemic and hypoxic preconditioning in cardiovascular and neurological tissue, in which mild stress confers a context-dependent benefit that is lost as stressor intensity increases. $CoCl_2$-mediated chemical stabilization of HIF-1α is a well-validated and widely adopted pharmacological approach for modeling hypoxic

signaling in vitro [ref], and our in vivo intermittent hypoxia model independently corroborated the same HIF-1α/ABCB1/BCL-2 axis under physiological oxygen restriction, reducing reliance on any single hypoxia-mimetic method.

The persistence of HIF-1α and ABCB1 expression under combination treatment indicates that the observed sensitization is unlikely to result from simple abrogation of hypoxia signaling, but the precise molecular intermediary linking moderate hypoxic stress to enhanced caspase-3 activation—whether through reactive oxygen species accumulation, metabolic substrate restriction following GLUT-1 suppression, or modulation of apoptotic threshold proteins—remains to be formally established through targeted pathway inhibition.

Limitations. First, the in vitro hypoxic model relied on $CoCl_2$-mediated chemical stabilization of HIF-1α, which, while a well-established and widely used approach, does not fully replicate the dynamic oxygen fluctuations of physiological hypoxia; this limitation was partially addressed by the complementary in vivo intermittent hypoxia model. Second, the KEGG pathway mapping presented here was based on a targeted panel of established hypoxia-associated markers rather than an unbiased, genome- or proteome-wide dataset, and should be interpreted as an illustrative framework of pathway interconnectivity rather than a comprehensive enrichment analysis.

5. CONCLUSION

In this study, we demonstrate that mild, intermittent hypoxia exerts a dual and context-dependent influence on breast cancer biology: in isolation, it reinforces a canonical HIF-1α-driven survival program characterized by elevated ABCB1/P-glycoprotein and BCL-2 expression and increased tumor growth, yet when combined with chemotherapy, it paradoxically enhances apoptotic commitment and suppresses tumor burden beyond what either intervention achieves alone. This biphasic relationship was consistently observed across complementary models—from chemical hypoxia in SKBR3 and MDA-MB-231 cells, where moderate $CoCl_2$ exposure (200 μM) maximized caspase-3 activation and GLUT-1 suppression under DOX/5-FU co-treatment, to the DMBA-induced rat mammary carcinoma model, where intermittent hypoxia combined with FUDOX chemotherapy produced the smallest tumors, the strongest apoptotic signal, and a significant survival benefit without evidence of systemic toxicity.

Collectively, these findings support a hormetic, threshold-dependent model of hypoxia–chemotherapy interaction, in which the same hypoxic signaling axis that promotes tumor survival in the absence of treatment becomes a vulnerability that chemotherapy can exploit when oxygen fluctuation is mild, intermittent, and bounded within an optimal range. This challenges the prevailing assumption that hypoxia uniformly drives chemoresistance and instead suggests that the relationship between tumor oxygenation and treatment response is non-linear and exposure-dependent. Future studies incorporating targeted HIF-1α inhibition or knockdown will be necessary to establish causality and to determine

whether controlled hypoxic conditioning could be leveraged as an adjunct strategy to improve chemotherapy efficacy in breast cancer.

6. CRediT authorship contribution statement

Nikolay Avtandilyan: Conceptualization, Methodology, Supervision, Project administration, Funding acquisition, Writing – review & editing.

Edita Nadiryan: Investigation, Methodology, Formal analysis, Validation.

Alina Maloyan: Conceptualization, Methodology, Supervision, Writing – review & editing.

Hayarpi Javrushyan: Conceptualization, Methodology, Investigation, Formal analysis, Data curation, Writing – original draft, Writing – review & editing.

7. Funding

This work was supported by the Higher Education and Science Committee of the Republic of Armenia (Grant No. 24WS-1F036).

8. Acknowledgements

The authors gratefully acknowledge Dr. Anna Grigoryan (Yerevan State University, Armenia) for providing access to the cryostat used in this study. The authors also thank Dr. Zara Karabekian (L.A. Orbeli Institute of Physiology, National Academy of Sciences of the Republic of Armenia) for generously providing the MDA-MB-231 and SK-BR-3 breast cancer cell lines used in this work. The authors are grateful to all members of the participating laboratories for their technical assistance and valuable scientific discussions throughout this study.

9. Ethics statement

All animal experiments were conducted in accordance with the European Directive 2010/63/EU for the protection of animals used for scientific purposes. The study protocol was reviewed and approved by the Armenian National Bioethics Association. All procedures were performed in accordance with institutional and national guidelines for the care and use of laboratory animals.

10. Declaration of Competing Interests

The authors declare that they have no known competing financial interests or personal relationships that could have appeared to influence the work reported in this paper.

11. Data availability

The data supporting the findings of this study are available from the corresponding author upon reasonable request.

12. Declaration of Generative AI and AI-assisted technologies in the writing process

During the preparation of this work, the author(s) used Claude (Anthropic) to assist with language editing, structuring, and refinement of the manuscript text. After using this tool, the author(s) reviewed and edited the content as needed and take full responsibility for the content of the published article.

13. REFERENCES

[1] K. Kannan, A. Srinivasan, A. Kannan, N. Ali, The Underlying Mechanisms and Emerging Strategies to Overcome Resistance in Breast Cancer, Cancers (Basel). 17 (2025). https://doi.org/10.3390/cancers17172938.

[2] L. Wilkinson, T. Gathani, Understanding breast cancer as a global health concern, British Journal of Radiology 95 (2022). https://doi.org/10.1259/BJR.20211033.

[3] H. Xu, J. Wen, J. Yang, S. Zhou, Y. Li, K. Xu, W. Li, S. Li, Tumor-microenvironment-on-a-chip: the construction and application, Cell Communication and Signaling 22 (2024). https://doi.org/10.1186/s12964-024-01884-4.

[4] Y. Zhao, C. Xing, Y. Deng, C. Ye, H. Peng, HIF-1α signaling: Essential roles in tumorigenesis and implications in targeted therapies, Genes Dis. 11 (2024) 234–251. https://doi.org/10.1016/j.gendis.2023.02.039.

[5] Q. Liu, V.A.C. Palmgren, E.H. Danen, S.E. Le Dévédec, Acute vs. chronic vs. intermittent hypoxia in breast Cancer: a review on its application in in vitro research, Mol. Biol. Rep. 49 (2022) 10961–10973. https://doi.org/10.1007/s11033-022-07802-6.

[6] G.L. Semenza, Hypoxia-inducible factors: Mediators of cancer progression and targets for cancer therapy, Trends Pharmacol. Sci. 33 (2012) 207–214. https://doi.org/10.1016/j.tips.2012.01.005.

[7] G.L. Semenza, Hypoxia-inducible factors in physiology and medicine, Cell 148 (2012) 399–408. https://doi.org/10.1016/j.cell.2012.01.021.

[8] V.M. Shah, B.C. Sheppard, R.C. Sears, A.W. Alani, Hypoxia: Friend or Foe for drug delivery in Pancreatic Cancer, Cancer Lett. 492 (2020) 63–70. https://doi.org/10.1016/j.canlet.2020.07.041.

[9] Y. Yuan, Z. Xiang, Y. Xia, J. Xie, X. Jiang, Z. Lu, The role of ATP binding cassette (ABC) transporters in breast cancer: Evaluating prognosis, predicting immunity, and guiding treatment, Channels 17 (2023). https://doi.org/10.1080/19336950.2023.2273247.

[10] L. Pang, Y. Cai, E.H.C. Tang, D. Yan, R. Kosuru, H. Li, M.G. Irwin, H. Ma, Z. Xia, Cox-2 Inhibition Protects against Hypoxia/Reoxygenation-Induced Cardiomyocyte Apoptosis via Akt-Dependent Enhancement of iNOS Expression, Oxid. Med. Cell. Longev. 2016 (2016). https://doi.org/10.1155/2016/3453059.

[11] S. Zhi, C. Chen, H. Huang, Z. Zhang, F. Zeng, S. Zhang, Hypoxia-inducible factor in breast cancer: role and target for breast cancer treatment, Front. Immunol. 15 (2024). https://doi.org/10.3389/fimmu.2024.1370800.

[12] J. Huang, L. Gao, B. Li, C. Liu, S. Hong, J. Min, L. Hong, Knockdown of Hypoxia-Inducible Factor 1α (HIF-1α) Promotes Autophagy and Inhibits Phosphatidylinositol 3-Kinase (PI3K)/AKT/ Mammalian

Target of Rapamycin (mTOR) Signaling Pathway in Ovarian Cancer Cells, Medical Science Monitor 25 (2019) 4250–4263. https://doi.org/10.12659/MSM.915730.

[13] T. Behrendt, R. Bielitzki, M. Behrens, F. Herold, L. Schega, Effects of Intermittent Hypoxia–Hyperoxia on Performance- and Health-Related Outcomes in Humans: A Systematic Review, Sports Med. Open 8 (2022). https://doi.org/10.1186/s40798-022-00450-x.

[14] A. Navarrete-Opazo, G.S. Mitchell, Therapeutic potential of intermittent hypoxia: a matter of dose Navarrete-Opazo A, Mitchell GS. Therapeutic potential of intermittent hypoxia: a matter of dose, Am J Physiol Regul Integr Comp Physiol 307 (2014) 1181–1197. https://doi.org/10.1152/ajpregu.00208.2014.-Intermittent.

[15] V. Damgaard, J. Mariegaard, J.M. Lindhardsen, H. Ehrenreich, K.W. Miskowiak, Neuroprotective Effects of Moderate Hypoxia: A Systematic Review, Brain Sci. 13 (2023). https://doi.org/10.3390/brainsci13121648.

[16] A. Ferrer, C.T. Roser, M.H. El-Far, V.H. Savanur, A. Eljarrah, M. Gergues, J.A. Kra, J.P. Etchegaray, P. Rameshwar, Hypoxia-mediated changes in bone marrow microenvironment in breast cancer dormancy, Cancer Lett. 488 (2020) 9–17. https://doi.org/10.1016/j.canlet.2020.05.026.

[17] R. Timon, I. Martinez-Guardado, F. Brocherie, Effects of Intermittent Normobaric Hypoxia on Health-Related Outcomes in Healthy Older Adults: A Systematic Review, Sports Med. Open 9 (2023). https://doi.org/10.1186/s40798-023-00560-0.

[18] A. Lequeux, M.Z. Noman, M. Xiao, D. Sauvage, K. Van Moer, E. Viry, I. Bocci, M. Hasmim, M. Bosseler, G. Berchem, B. Janji, Impact of hypoxic tumor microenvironment and tumor cell plasticity on the expression of immune checkpoints, Cancer Lett. 458 (2019) 13–20. https://doi.org/10.1016/j.canlet.2019.05.021.

[19] X. He, J. Wang, W. Wei, M. Shi, B. Xin, T. Zhang, X. Shen, Hypoxia regulates ABCG2 activity through the activivation of ERK1/2/HIF-1α and contributes to chemoresistance in pancreatic cancer cells, Cancer Biol. Ther. 17 (2016) 188–198. https://doi.org/10.1080/15384047.2016.1139228.

[20] T. Luo, D. Wang, L. Liu, Y. Zhang, C. Han, Y. Xie, Y. Liu, J. Liang, G. Qiu, H. Li, D. Su, J. Liu, K. Zhang, Switching Reactive Oxygen Species into Reactive Nitrogen Species by Photocleaved O2-Released Nanoplatforms Favors Hypoxic Tumor Repression, Advanced Science 8 (2021). https://doi.org/10.1002/advs.202101065.

[21] M. Ginovyan, H. Javrushyan, S. Hovhannisyan, E. Nadiryan, G. Sevoyan, T. Harutyunyan, S. Gevorgyan, Z. Karabekian, A. Maloyan, N. Avtandilyan, 5-fluorouracil and Rumex obtusifolius extract combination trigger A549 cancer cell apoptosis: uncovering PI3K/Akt inhibition by in vitro and in silico approaches, Sci. Rep. 14 (2024). https://doi.org/10.1038/s41598-024-65816-5.

[22] C. Ooppachai, P. Limtrakul, S. Yodkeeree, Dicentrine potentiates TNF-α-induced apoptosis and suppresses invasion of a549 lung adenocarcinoma cells via modulation of nf-κb and ap-1 activation, Molecules 24 (2019). https://doi.org/10.3390/molecules24224100.

[23] M. Segatto, E. Fico, M. Gharbiya, P. Rosso, V. Carito, P. Tirassa, R. Plateroti, A. Lambiase, VEGF inhibition alters neurotrophin signalling pathways and induces caspase-3 activation and autophagy in rabbit retina, J. Cell. Physiol. 234 (2019) 18297–18307. https://doi.org/10.1002/jcp.28462.

[24] H. Javrushyan, M. Ginovyan, T. Harutyunyan, S. Gevorgyan, Z. Karabekian, A. Maloyan, N. Avtandilyan, Elucidating the impact of Hypericum alpestre extract and L-NAME on the PI3K/Akt signaling pathway in A549 lung adenocarcinoma and MDA-MB-231 triple-negative breast cancer cells, PLoS One 20 (2025) e0303736. https://doi.org/10.1371/journal.pone.0303736.

[25] H. Javrushyan, G. Petrosyan, M. Mróz, B. Kusznierewicz, Y. Alharithi, M. Ginovyan, A. Maloyan, N. Avtandilyan, Evaluating the Efficacy of Polyphenol-Enriched Plant Extracts and Pathway Modulators in

the Bone Marrow to Suppress Breast Cancer Progression, The FASEB Journal 40 (2026). https://doi.org/10.1096/fj.202501773RRR.

[26] N. Avtandilyan, H. Javrushyan, M. Ginovyan, A. Karapetyan, A. Trchounian, Anti-cancer effect of in vivo inhibition of nitric oxide synthase in a rat model of breast cancer, Mol. Cell. Biochem. 478 (2023) 261–275. https://doi.org/10.1007/s11010-022-04489-y.

[27] M. Ginovyan, S. Gevorgyan, H. Javrushyan, B. Kusznierewicz, I. Koss-Mikołajczyk, N. Sahakyan, A. Bartoszek, N. Avtandilyan, Inhibition of the PI3K signaling pathway in cancer cells by Agrimonia eupatoria L. ethanolic extract: identification of tricoumaroyl spermidine as a potential PI3K inhibitor, BMC Complement. Med. Ther. (2026). https://doi.org/10.1186/s12906-025-05231-z.

[28] D. Tang, M. Chen, X. Huang, G. Zhang, L. Zeng, G. Zhang, S. Wu, Y. Wang, SRplot: A free online platform for data visualization and graphing, PLoS One 18 (2023). https://doi.org/10.1371/journal.pone.0294236.

[29] Y. Hao, M. Xin, L. Feng, X. Wang, X. Wang, D. Ma, J. Feng, Review Cerebral Ischemic Tolerance and Preconditioning: Methods, Mechanisms, Clinical Applications, and Challenges, Front. Neurol. 11 (2020). https://doi.org/10.3389/fneur.2020.00812.

[30] E.J. Calabrese, L.A. Baldwin, Defining hormesis, Hum. Exp. Toxicol. 21 (2002) 91–97. https://doi.org/10.1191/0960327102ht217oa.

[31] L. Yong, S. Tang, H. Yu, H. Zhang, Y. Zhang, Y. Wan, F. Cai, The role of hypoxia-inducible factor-1 alpha in multidrug-resistant breast cancer, Front. Oncol. 12 (2022). https://doi.org/10.3389/fonc.2022.964934.

[32] S. Doublier, D.C. Belisario, M. Polimeni, L. Annaratone, C. Riganti, E. Allia, D. Ghigo, A. Bosia, A. Sapino, HIF-1 activation induces doxorubicin resistance in MCF7 3-D spheroids via P-glycoprotein expression: a potential model of the chemo-resistance of invasive micropapillary carcinoma of the breast, 2011. http://www.biomedcentral.com/1471-2407/12/4.

[33] Y. Lv, S. Zhao, J. Han, L. Zheng, Z. Yang, L. Zhao, Hypoxia-inducible factor-1α induces multidrug resistance protein in colon cancer, Onco. Targets. Ther. 8 (2015) 1941–1948. https://doi.org/10.2147/OTT.S82835.

[34] S.C. Bondy, The Hormesis Concept: Strengths and Shortcomings, Biomolecules 13 (2023). https://doi.org/10.3390/biom13101512.

[35] B. Le, A. Cressman, D. Morales, F.A. Fierro, First Clinical Experiences Using Preconditioning Approaches to Improve MSC-Based Therapies, Curr. Stem Cell Rep. 10 (2024) 1–7. https://doi.org/10.1007/s40778-023-00232-5.

[36] S. Nong, X. Han, Y. Xiang, Y. Qian, Y. Wei, T. Zhang, K. Tian, K. Shen, J. Yang, X. Ma, Metabolic reprogramming in cancer: Mechanisms and therapeutics, MedComm (Beijing). 4 (2023). https://doi.org/10.1002/mco2.218.

[37] S. Liu, X. Zhang, W. Wang, X. Li, X. Sun, Y. Zhao, Q. Wang, Y. Li, F. Hu, H. Ren, Metabolic reprogramming and therapeutic resistance in primary and metastatic breast cancer, Mol. Cancer 23 (2024). https://doi.org/10.1186/s12943-024-02165-x.

[38] Q. Wu, W. ba-alawi, G. Deblois, J. Cruickshank, S. Duan, E. Lima-Fernandes, J. Haight, S.A.M. Tonekaboni, A.M. Fortier, H. Kuasne, T.D. McKee, H. Mahmoud, M. Kushida, S. Cameron, N. Dogan-Artun, W.J. Chen, Y. Nie, L.X. Zhang, R.N. Vellanki, S. Zhou, P. Prinos, B.G. Wouters, P.B. Dirks, S.J. Done, M. Park, D.W. Cescon, B. Haibe-Kains, M. Lupien, C.H. Arrowsmith, GLUT1 inhibition blocks growth of RB1-positive triple negative breast cancer, Nat. Commun. 11 (2020). https://doi.org/10.1038/s41467-020-18020-8.

[39] W.R. Wilson, M.P. Hay, Targeting hypoxia in cancer therapy, Nat. Rev. Cancer 11 (2011) 393–410. https://doi.org/10.1038/nrc3064.

[40] S.S. Chung, Y. Wu, Q. Okobi, D. Adekoya, M. Atefi, O. Clarke, P. Dutta, J. V. Vadgama, Proinflammatory Cytokines IL-6 and TNF- α Increased Telomerase Activity through NF- κ B/STAT1/STAT3 Activation, and Withaferin A Inhibited the Signaling in Colorectal Cancer Cells, Mediators Inflamm. 2017 (2017). https://doi.org/10.1155/2017/5958429.